frontiers in Chemistry

ORIGINAL RESEARCH
published: 27 July 2021
doi: 10.3389/fchem.2021.700380

Effects of Different Delocalized π-Conjugated Systems Towards the TiO_2-Based Hybrid Photocatalysts

Weibo Zhang[1], Pinghua Chen[2,3], Jun Liu[2,3], NanNan Huang[4], Chenglian Feng[4], Daishe Wu[1] and Yingchen Bai[4]**

[1]Key Laboratory of Poyang Lake Environment and Resource Utilization, Ministry of Education, School of Resources Environmental and Chemical Engineering, Nanchang University, Nanchang, China, [2]Key Laboratory of Jiangxi Province for Persistent Pollutants Control and Resources Recycle, Nanchang, China, [3]College of Environmental and Chemical Engineering, Nanchang Hangkong University, Nanchang, China, [4]State Key Laboratory of Environmental Criteria and Risk Assessment, Chinese Research Academy of Environmental Sciences, Beijing, China

Modulating the structure of a photocatalyst at the molecular level can improve the photocatalytic efficiency and provides a guide for the synthesis of highly qualified photocatalysts. In this study, TiO_2 was modified by various organic compounds to form different TiO_2-based hybrid photocatalysts. 1,10-Phenanthroline (Phen) is an organic material with delocalized π-conjugated systems. It was used to modify TiO_2 to form the hybrid photocatalyst Phen/TiO_2. Furthermore, 1,10-phenanthrolin-5-amine (Phen-NH_2) and 1,10-phenanthroline-5-nitro (Phen-NO_2) were also used to modify TiO_2 to form NH_2-Phen/TiO_2 and NO_2-Phen/TiO_2, respectively. The samples of TiO_2, Phen/TiO_2, NO_2-Phen/TiO_2, and NH_2-Phen/TiO_2 were carefully characterized, and their photocatalytic performance was compared. The results indicated that the photocatalytic efficiency followed the order of NH_2-Phen/TiO_2 > NO_2-Phen/TiO_2 > Phen/TiO_2 > TiO_2. It could be found that modifying TiO_2 with different organic compounds containing delocalized π-conjugated systems could enhance the photocatalytic ability; furthermore, the level of this enhancement could be modulated by different delocalized π-conjugated systems.

Keywords: π-conjugated systems, photocatalyst, phenanthroline, derivatives of phenanthroline, TiO_2

OPEN ACCESS

Edited by:
Yanbiao Liu,
Donghua University, China

Reviewed by:
Qingyi Zeng,
University of South China, China
Chensi Shen,
Donghua University, China

****Correspondence:***
Daishe Wu
dswu@ncu.edu.cn
Yingchen Bai
baiyc@craes.org.cn

Specialty section:
This article was submitted to Green and Sustainable Chemistry, a section of the journal Frontiers in Chemistry

Received: *26 April 2021*
Accepted: *01 June 2021*
Published: *27 July 2021*

Citation:
Zhang W, Chen P, Liu J, Huang N, Feng C, Wu D and Bai Y (2021) Effects of Different Delocalized π-Conjugated Systems Towards the TiO_2-Based Hybrid Photocatalysts. Front. Chem. 9:700380. doi: 10.3389/fchem.2021.700380

INTRODUCTION

Wastewater is a serious environmental problem as it contains a large number of hazardous organic compounds, such as polycyclic aromatic hydrocarbons, pharmaceuticals (PhACs), and organic dyes (Grzechulska-Damszel et al., 2009; Kim et al., 2013; Li et al., 2018; Murgolo et al., 2021). Therefore, there is an urgent need to find a technology to deal with these pollution problems. Photocatalysis is a green and efficient technique, which has become significant in the field of environmental science because it can utilize the renewable solar energy for the removal of organic pollutants in wastewater (Chen et al., 2010; Chong et al., 2010; Kubacka et al., 2012; Yang et al., 2018). Titanium dioxide (TiO_2) is one of the most important photocatalysts due to its environment-friendly nature, non-toxicity, chemical stability, and low cost (Liu et al., 2009; Awfa et al., 2018; Gopinath et al., 2020). However, TiO_2 still has two major disadvantages: one is that pure TiO_2 has a large band gap (e.g., = 3.0–3.2 eV), which means TiO_2 can absorb only the ultraviolet light in the photocatalytic reaction, and the other is its high recombination rate of photoinduced electron–hole pairs (Cottineau et al.,

2014; Pang et al., 2016; Murgolo et al., 2021). Thus, there is an urgent need to improve the quantum efficiency and light response range of titanium dioxide by modification.

Recently, surface decoration, such as surface coating with metallic oxide, dye grafting on a TiO_2 surface, and introducing an organic π-conjugated system into the surface, has been developed for reducing the electron–hole recombination rate and increasing the range or intensity of light absorbed by TiO_2 (Kaur and Singh, 2007; Carbuloni et al., 2020; Xu et al., 2021). The main reason behind the development of surface decoration is that some special structures such as heterojunctions or π-conjugated systems are formed between TiO_2 and the foreign substance, which can alter the interfacial charge-transfer (ICT) dynamics between TiO_2 and its surface materials (Ardo and Meyer, 2009; Jono et al., 2011; Fujisawa et al., 2016). The interfacial charge-transfer (ICT) involved in the interface interaction between wide band gap inorganic semiconductors such as TiO_2 and organic materials have attracted increasing attention due to being beneficial to absorption of visible light and direct electron-injection to TiO_2 (Ramakrishna and Ghosh, 2002; Verma and Ghosh, 2014; Fujisawa et al., 2017). Furthermore, some new organic molecules that contain a donor–π–acceptor (D-π-A) structure extend the intramolecular charge-transfer time and distance, providing more opportunities for the synthesis of highly efficient photochemical materials (Edvinsson et al., 2007; Tian et al., 2008; Cai et al., 2011). The π-conjugated system modified by functionalized groups such as electron-donating/withdrawing groups has been developed for modifying the electronic structure of organic compounds, which affect the performance of catalysts (Shibano et al., 2007; Verma and Ghosh, 2014; Margalias et al., 2015; Xie et al., 2020). Therefore, it is necessary to analyze the relationship between the organic material that is modified by functionalized groups and the activity of TiO_2 and light, which help synthesize highly efficient TiO_2-based catalysts to achieve efficient photocatalytic degradation of organic pollutants in water.

1,10-Phenanthroline (Phen) and its derivatives have a wide range of application in areas such as synthesis of conjugated organic materials due to their high charge-transfer mobility and good electro/photoactive properties (Wei et al., 2018; Çakar, 2019). In this work, 1,10-phenanthroline (Phen), 1,10-phenanthrolin-5-amine (Phen-NH_2), and 1,10-phenanthroline-5-nitro (Phen-NO_2) were used to modify TiO_2 to form Phen/TiO_2, NH_2-Phen/TiO_2, and NO_2-Phen/TiO_2, respectively. The morphology, structure, and photoelectric property of the as-prepared photocatalysts were characterized. Their photocatalytic activity was evaluated by photodegradation of methyl orange (MO) under visible light irradiation. The effects of various conjugated systems on their visible light photocatalytic activity were also investigated. This study provides a guide for the synthesis of highly efficient TiO_2-based catalysts to achieve efficient photocatalytic degradation of organic pollutants in water.

EXPERIMENT

Catalyst Preparation

Synthesis of Phen-NO_2 and Phen-NH_2

All starting materials were purchased in an analytically pure form from Aladdin Chemical Reagent Co., Ltd. and utilized without further purification. Phen-NO_2 and Phen-NH_2 were prepared following the method in our previous work (Jiang et al., 2016). Typically, to a solution of H_2SO_4, phenanthroline was added at room temperature and then a mixture of H_2SO_4 and HNO_3 (1:1) was slowly added. The resulting mixture was refluxed for 3 h, and Phen-NO_2 was obtained after recrystallization with ethanol. Phen-NO_2 was reduced to Phen-NH_2 with hydrazine hydrate. The synthetic routes and structures of phenanthroline, Phen-NO_2, and Phen-NH_2 are shown in **Figure 1**.

Synthesis of NH_2-Phen/TiO_2, NO_2-Phen/TiO_2, Phen/TiO_2, and TiO_2

Typically, 3 ml of titanium tetrabutoxide (TBOB) and 0.44 mmol of Phen-NH_2 were added into 20 ml of ethanol and stirred for 30 min to form a uniform solution. Then, 50 ml of deionized water was added in drops, and the solution was continuously stirred for another 1 h. Then, the mixture was transferred to a Teflon-lined stainless-steel autoclave and maintained at 180°C for 24 h. Finally, the NH_2-Phen/TiO_2 obtained after centrifugation was washed with ethanol and deionized water several times and dried in a vacuum oven at 60°C for 12 h. NO_2-Phen/TiO_2 and Phen/TiO_2 were prepared by the method described above in which Phen-NO_2 and Phen replaced Phen-NH_2. Bare TiO_2 was also prepared by the same method without the addition of organic compounds.

Characterization

The morphologies of the powders were analyzed by using a scanning electron microscope (SEM) (Japanese JEOL JSM-6360). X-ray diffraction (XRD) was performed by using a D8 X-ray diffractometer. The ultraviolet–visible (UV–Vis) diffuse reflectance spectra (DRS) were obtained by using a UV-Vis NIR spectrometer (Lambda 900). The fluorescence spectrum was measured by using a fluorescence spectrometer (F-7000, Japan). Electrochemical impedance and Mott–Schottky curves were recorded on an electrochemical workstation (CHI660C, Shanghai Chenhua, China) with a standard three-electrode system at room temperature. Photoluminescence spectra (PL) were recorded on an F-7000 fluorescence spectrophotometer (Hitachi, Japan).

Photocatalytic Experiments

The photocatalytic activity of all as-prepared catalysts was evaluated by the degradation of MO under visible light irradiation. The light source was a 500-W Xe illuminator (PerfectLight, Beijing, China). In each experiment, 70 mg of the catalyst was added into 70 ml of MO solution (10 mg/L) in a clean beaker. Before illumination, the suspension was stirred for 30 min in the dark, resulting in a quick adsorption saturation. Then, the suspension was exposed to visible light irradiation with

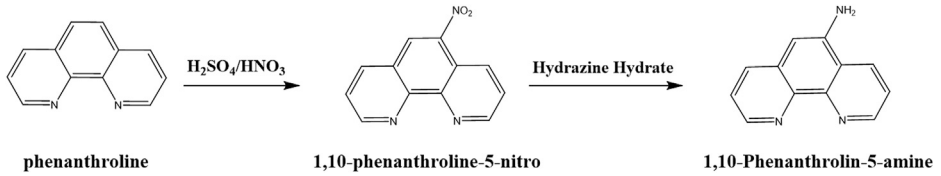

FIGURE 1 | The synthetic routes and structures of phenanthroline, Phen-NO_2, and Phen-NH_2.

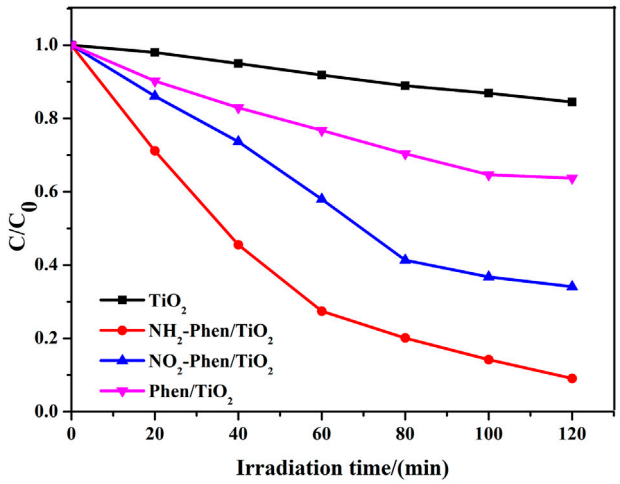

FIGURE 2 | Photoreduction of MO over the as-prepared materials under visible light (70 mg catalysts and 70 ml MO solution with a concentration of 10 mg/L).

magnetic stirring. At the given time intervals, the suspension was sampled and the photocatalytic particles were removed from the solution using a membrane filter. The concentration of MO in the solution was measured by its absorption intensity at 464 nm.

RESULTS AND DISCUSSION

The degradation rates of methyl orange (MO) adsorbed on the catalysts under visible light in 120 min are illustrated in **Figure 2**. NH_2-Phen/TiO_2, NO_2-Phen/TiO_2, and Phen/TiO_2 showed higher photocatalytic activity than bare TiO_2, indicating that Phen, Phen-NH_2, and Phen-NO_2 significantly improved the photocatalytic activity in the composites. As shown in **Supplementary Figure S1**, TiO_2 has almost no adsorption capacity toward MO. The adsorption capacity of modified TiO_2 significantly increases and reaches adsorption saturation within 30 min. The final adsorption capacity of NO_2-Phen/TiO_2 and NH_2-Phen/TiO_2 is almost stable, which is lower than that of Phen/TiO_2. However, the catalytic efficiency of NO_2-Phen/TiO_2 and NH_2-Phen/TiO_2 is higher than that of Phen/TiO_2, indicating that photodegradation is the main reason for MO removal. The catalytic efficiency of NH_2-Phen/TiO_2 is the highest (91%), which is nearly 2.5 times and 5.7 times that of Phen/TiO_2 (36%) and bare TiO_2 (16%), respectively. NO_2-Phen/TiO_2 has the second highest catalytic efficiency (66%), which is nearly 1.8 times and 4.1 times that of Phen/TiO_2 and bare TiO_2, respectively. These results showed that the delocalized π-conjugated system with the amino group is more conducive to photodegradation of MO. It is reported that the electron-donating group can induce HOMO-LUMO electronic transitions that cause a change in the dipole moment, which results in effective separation of photogenerated charges (Belviso et al., 2019; Li et al., 2020). Therefore, it is notable that the catalytic efficiency followed the order of NH_2-Phen/TiO_2 > NO_2-Phen/TiO_2 > Phen/TiO_2, which indicates that $-NH_2$ has a strong electron-donating group than $-NO_2$.

Figure 3 shows scanning electron microscopic (SEM) images of NH_2-Phen/TiO_2, NO_2-Phen/TiO_2, Phen/TiO_2, and TiO_2, indicating that the morphologies of NH_2-Phen/TiO_2, NO_2-Phen/TiO_2, and Phen/TiO_2 are not significantly different than that of bare TiO_2. All these samples show similar morphologies with irregular nanoparticles, which means that the preparation methods cannot obviously change the morphologies of TiO_2 particles. Furthermore, severe agglomeration of the TiO_2 nanoparticles is also detected, while the modified TiO_2 nanoparticles have better dispersion, indicating that the modification of TiO_2 with Phen and its derivatives is beneficial to the dispersion of the nanoparticles. It was reported that the catalytic activity was related to the dispersion of the nanoparticles because a better dispersion could result in a better exposure of active sites (Xun et al., 2020). Therefore, improved dispersion may be another reason for the improved catalytic activity of the modified TiO_2 catalysts.

X-ray diffraction (XRD) was used to analyze the structure of the catalysts. **Figure 4A** shows the XRD patterns of NH_2-Phen/TiO_2, NO_2-Phen/TiO_2, Phen/TiO_2, and bare TiO_2. The diffraction peaks of bare TiO_2 observed at 25.2°, 37.8°, 48.0°, 53.9°, 55.0°, and 62.6° are consistent with anatase TiO_2 (101), (004), (200), (105), (211), and (204) lattice planes (JCPDS Card No. 21-1272), respectively. While comparing the diffraction peaks of TiO_2, Phen/TiO_2, NO_2-Phen/TiO_2, and NH_2-Phen/TiO_2, all show two new characteristic peaks at 2θ of 30.7° and 36.2°, which correspond to the (211) plane of titanite TiO_2 and the (101) plane of rutile TiO_2, respectively. This indicates that the modification of Phen, Phen-NO_2, and Phen-NH_2 has caused two new phase structures of brookite TiO_2 and rutile TiO_2 appear in NH_2-Phen/TiO_2, NO_2-Phen/TiO_2, and Phen/TiO_2 along with the anatase TiO_2 phase. These results indicate that the modification of Phen and its derivatives is beneficial for forming brookite TiO_2 and results in a mixed phase of anatase, brookite, and rutile TiO_2 in the catalysts. The changes in crystalline phases imply the successful modification of Phen and its derivatives.

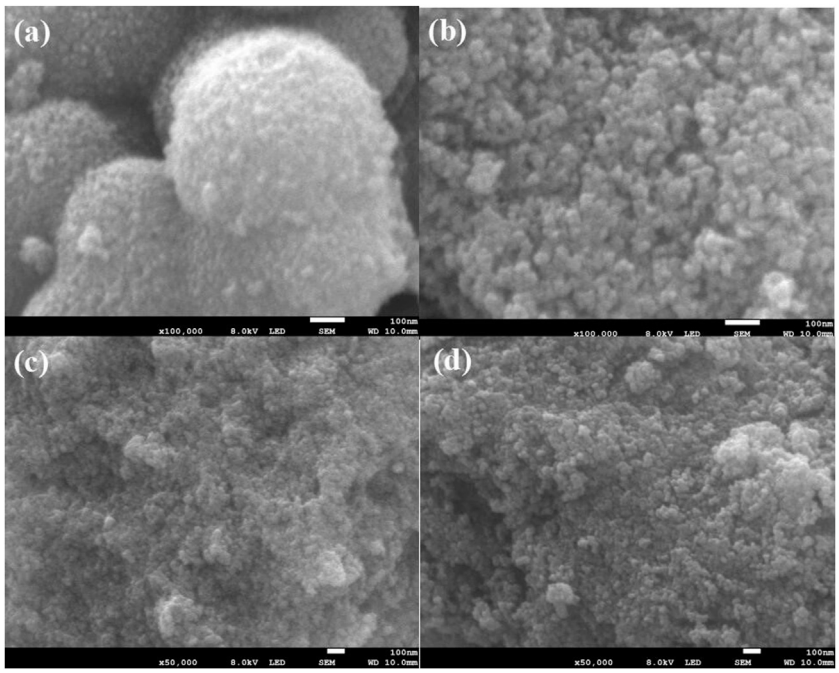

FIGURE 3 | SEM image of TiO_2 **(A)**, Phen/TiO_2 **(B)**, NO_2-Phen/TiO_2 **(C)**, and NH_2-Phen/TiO_2 **(D)**.

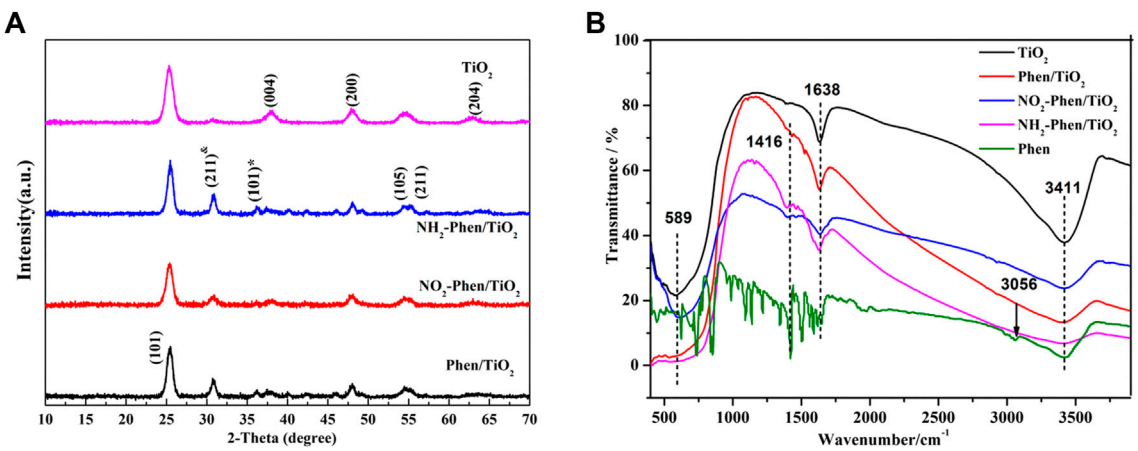

FIGURE 4 | XRD **(A)** and FT-IR patterns **(B)** of TiO_2, Phen/TiO_2, NO_2-Phen/TiO_2, and NH_2-Phen/TiO_2.

Furthermore, a mixture of different crystalline phases could give rise to a higher photocatalytic activity (Dai et al., 2015; Kandiel et al., 2013). According to the Scherrer formula (Cao et al., 2011), the lattice sizes of TiO_2, Phen/TiO_2, NO_2-Phen/TiO_2, and NH_2-Phen/TiO_2 are 9.35, 11.03, 10.82, and 9.44 nm, respectively.

Infrared characterization was performed to determine the functional groups present in the catalysts. **Figure 4B** shows the FT-IR spectral data of NH_2-Phen/TiO_2, NO_2-Phen/TiO_2, Phen/TiO_2, and TiO_2. The peaks at 589 cm^{-1} and 1638 cm^{-1} are attributed to the vibration of Ti–O–Ti (Xu et al., 2010) and stretching vibration of C=N of Phen (Li et al., 2016), respectively. After different groups were introduced into Phen/TiO_2, NO_2-Phen/TiO_2, and NH_2-Phen/TiO_2, the infrared absorption peaks of these groups were also observed. The antisymmetric stretching vibration of $-NO_2$ was observed at 1,584 cm^{-1}; the ν(N-H) bands of $-NH_2$ were observed at 1,416 and 3,411 cm^{-1} (Li et al., 2016). These results indicate that the corresponding derivatives of Phen are successfully combined with TiO_2. As noted in the FT-IR spectrum, the C=C stretching band at 1,520 cm^{-1} of Phen/TiO_2 shifted to 1,462–1,470 cm^{-1} of NO_2-Phen/TiO_2 and NH_2-Phen/TiO_2, indicating that the $-NO_2$ and $-HN_2$ groups increase the conjugation length of Phen (Feng et al., 2005). Meanwhile, the

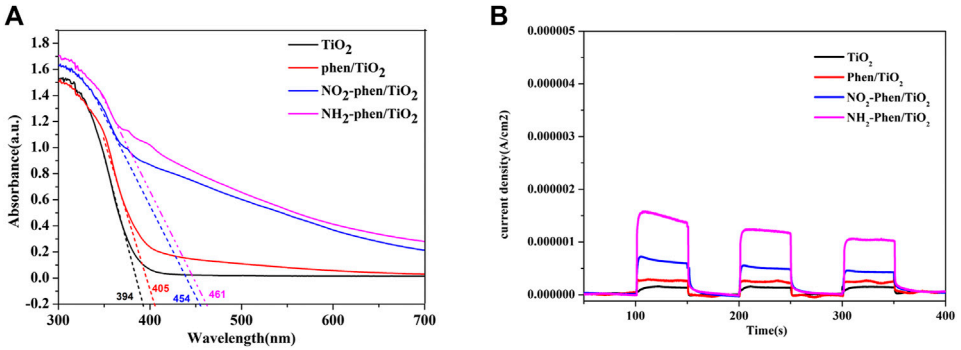

FIGURE 5 | UV–Vis spectra **(A)** and photocurrent response **(B)** of NH_2-Phen/TiO_2, NO_2-Phen/TiO_2, Phen/TiO_2, and TiO_2.

peak of NH_2-Phen/TiO_2, NO_2-Phen/TiO_2, and Phen-TiO_2 has redshifted compared with that of TiO_2, which may be due to the strong interaction between TiO_2 and the derivatives of Phen.

Figure 5A shows the UV–Vis diffuse reflectance spectra (DRS) of NH_2-Phen/TiO_2, NO_2-Phen/TiO_2, Phen-TiO_2, and bare TiO_2. It can be seen from the figure that the absorption edges of all NH_2-Phen/TiO_2, NO_2-Phen/TiO_2, and Phen-TiO_2 catalysts exhibit an obvious redshift to a higher wavelength, and the intensities are stronger in the visible range than that of TiO_2. It can be indicated that the response range of TiO_2 under visible light has been broadened after the modification of TiO_2 by Phen and its derivatives. In addition, the redshift of the absorption edge indicates the decrease in band gap energy (Luo et al., 2013), and the band gap of all catalysts can be calculated as follows (Xu et al., 2018):

$$E_g = 1240/\lambda_g, \tag{1}$$

where E_g and λ_g are the band gap energy and absorption edge of the photocatalyst, respectively. The absorption edge of TiO_2, Phen/TiO_2, NO_2-Phen/TiO_2, and NH_2-Phen/TiO_2 is approximately 394, 405, 454, and 461 nm, respectively. Consequently, the band gap energy (EG) of TiO_2, Phen/TiO_2, NO_2-Phen/TiO_2, and NH_2-Phen/TiO_2 is 3.15, 3.06, 2.73, and 2.69 eV, respectively. Thus, NH_2-Phen/TiO_2 has the largest redshift and the narrowest band gap energy, and the redshift and EG are in the order of NH_2-Phen/TiO_2 > NO_2-Phen/TiO_2 > Phen/TiO_2, which is consistent with the result of the photocatalytic degradation. Based on this, we indicate that introducing a delocalized π-conjugated system with the amino group into TiO_2 has a significant effect on the optical performance of the photocatalyst.

The photocurrent responses of the four catalysts under visible light irradiation are shown in **Figure 5B**. It is notable that the photocurrent intensity value of NH_2-Phen/TiO_2 after stabilization is about 1.0 μA, which is significantly higher than that of the other samples, indicating higher efficient charge-carrier separation at the interface of NH_2-Phen/TiO_2 (Jiang et al., 2018; Wu et al., 2018). The stronger photocurrent intensity indicates that the generation, separation, and transfer efficiency of NH_2-Phen/TiO_2-photogenerated electron–hole pairs are higher, and the recombination rate of electron–hole pairs is lower. At the same time, the photocurrent intensity value of NO_2-Phen/TiO_2, Phen/TiO_2, and TiO_2 is about 0.44, 0.28, and 0.14 μA, respectively. The results are in the order of NH_2-Phen/TiO_2 > NO_2-Phen/TiO_2 > Phen/TiO_2, which is consistent with the results of the photocatalytic degradation and the DRS.

The separation of photoinduced electron–hole pairs is important for photocatalysis and can be explored from photoluminescence (PL) spectroscopy (Zhou et al., 2018). As shown in **Figure 6A**, the PL intensities of all Phen/TiO_2, NO_2-Phen/TiO_2, and NH_2-Phen/TiO_2 are lower that of bare TiO_2, indicating that the modification of Phen and its derivatives can suppress the recombination of electron–hole pairs, because higher PL intensity implies more drastic recombination of charge carriers, which favor the photocatalytic reactions. Comparing the PL intensity of the photocatalysts in **Figure 6A**, it is not difficult to speculate that the recombination rate of electron–hole pairs is in the order of Phen/TiO_2 > NO_2-Phen/TiO_2 > NH_2-Phen/TiO_2, which indicates that a delocalized π-conjugated system with the amino group is more conducive to suppress the recombination of electron–hole pairs. Subsequently, the electrochemical impedance spectra (EIS) are obtained to investigate the charge transport properties of Phen/TiO_2, NO_2-Phen/TiO_2, NH_2-Phen/TiO_2, and bare TiO_2. As shown in **Figure 6B**, NH_2-Phen/TiO_2 has the smallest arc radius and Phen/TiO_2 has the largest arc radius except bare TiO_2 (Dai et al., 2015). The smallest arc radius implies the fastest interfacial charge-transfer properties, which facilitates subsequent photocatalytic reactions. The photocatalytic performance speculated by PL and EIS is in the order of NH_2-Phen/TiO_2 > NO_2-Phen/TiO_2 > Phen/TiO_2, which is consistent with the result of the photocatalytic degradation experiment.

Figure 7 shows the Mott–Schottky plots of bare TiO_2 and Phen/TiO_2, NO_2-Phen/TiO_2, and NH_2-Phen/TiO_2, and all the catalysts have positive slopes of Mott–Schottky plots, indicating that these catalysts are n-type semiconductors (Zhang and Cheng, 2009). According to the tangent line of the Mott–Schottky curve (**Figure 7**), the calculated flat-band potential energy V_{fb} of NH_2-Phen/TiO_2, NO_2-Phen/TiO_2, Phen/TiO_2, and TiO_2 is −0.51, −0.48, −0.46, and −0.40 eV vs. SCE and −0.27, −0.25, −0.23, and −0.21 eV vs. SHE, respectively. In general, as an n-type

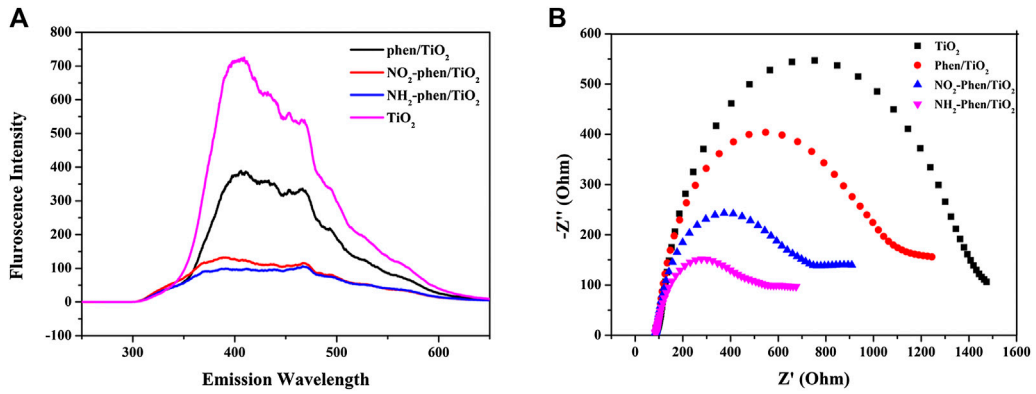

FIGURE 6 | Photoluminescence spectra **(A)** and electrochemical impedance spectroscopy **(B)** of NH_2-Phen/TiO_2, NO_2-Phen/TiO_2, Phen/TiO_2, and TiO_2.

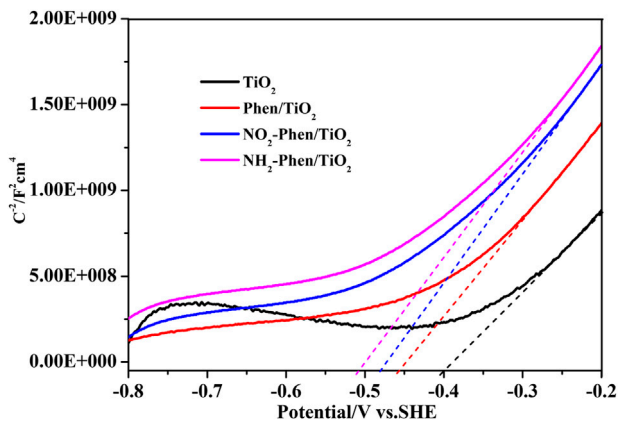

FIGURE 7 | Mott–Schottky plots of TiO_2, Phen/TiO_2, NO_2-Phen/TiO_2, and NH_2-Phen/TiO_2.

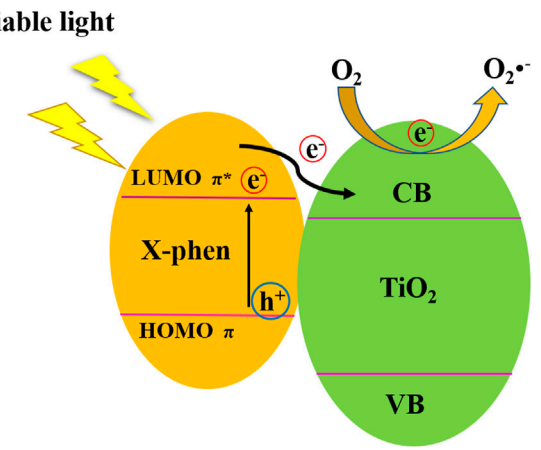

FIGURE 9 | Possible visible light photocatalytic mechanism of NH_2-Phen/TiO_2, NO_2-Phen/TiO_2, and Phen/TiO_2 nanoparticles.

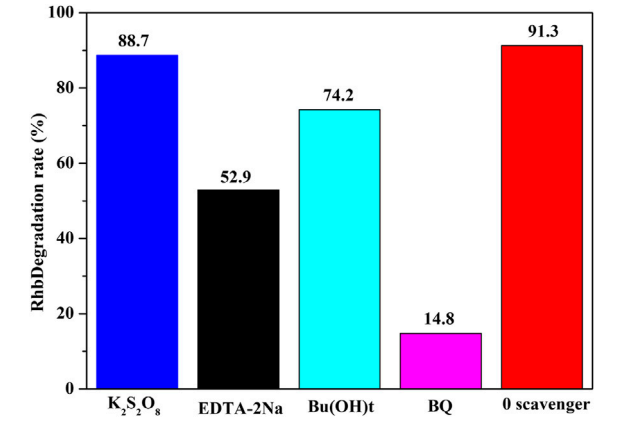

FIGURE 8 | Photocatalytic degradation of MO by NH_2-Phen/TiO_2 in the presence of different capture agents under visible light (70 mg catalysts and 70 ml MO solution with a concentration of 10 mg/L).

semiconductor, the flat-band potential energy is equal to its Fermi level, while the conduction band (CB) potential is approximately 0.2 eV less than its Fermi level (Ishikawa et al., 2002; Zhou et al., 2011). Thus, E_{CB} of NH_2-Phen/TiO_2, NO_2-Phen/TiO_2, Phen/TiO_2, and TiO_2 is −0.47, −0.45, −0.43, and −0.41 eV vs. SHE, respectively. According to the E_G value estimated by DRS and the empirical formula ($E_G = E_{VB} - E_{CB}$), the corresponding valence band (VB) potentials can be calculated as 2.22, 2.28, 2.63, and 2.74 eV, respectively.

To understand the possible mechanism for the improved photocatalytic activity of NH_2-Phen/TiO_2, trapping experiments were performed to identify the active species for the photodegradation (Zou et al., 2016; Dong et al., 2017). There are four active species (e^-, h^+, •OH radicals, and $•O_2^-$ radicals that can be captured by t-BuOH, $K_2S_2O_8$, DETA-2Na, and BQ, respectively) that play important roles in the photocatalytic reaction process (Jiang et al., 2018). As seen in **Figure 8**, the photocatalytic degradation rate of MO under visible light without any trapping agent is 91.3%, while the degradation efficiency of MO by adding t-BuOH, $K_2S_2O_8$, DETA-2Na, and BQ is 74.2,

88.7, 52.9, and 14.8%, respectively. These results indicate that $\bullet O_2^-$ is the main active species responsible for the degradation of MO and h^+ is the secondary active species. According to the results of the Mott–Schottky analysis, the E_{CB} and valence potential of NH_2-Phen/TiO_2 are approximately −0.47 eV vs. SHE and 2.22 eV vs. SHE, which are lower than the reduction potential of $O_2/\bullet O_2^-$ (−0.33 V) and •OH/OH (2.38 V) (Shao et al., 2015). Therefore, when NH_2-Phen/TiO_2 is irradiated by visible light during the period of photodegradation of MO, O_2 is reduced to $\bullet O_2^-$ by electrons, while OH^- cannot be oxidized to •OH by holes.

On the basis of the above results, the possible mechanism of NH_2-Phen/TiO_2, NO_2-Phen/TiO_2, and Phen/TiO_2 photocatalytic degradation of methyl orange (MO) is proposed in **Figure 9**. Phen and its derivatives can greatly promote the dispersion of the nanoparticles, resulting in more active sites to be exposed. Furthermore, Phen and its derivatives can act as sensitizers to enhance visible light absorption. Under the irradiation of visible light, the delocalized π-conjugated Phen and its derivatives on the surface of NH_2-Phen/TiO_2, NO_2-Phen/TiO_2, and Phen/TiO_2 nanocomposites can easily absorb visible light to induce a π–π^* transition state and then generate electron–hole pairs. The excited electrons in the LUMO of Phen and its derivatives will be easily injected into the conduction band of TiO_2. A fast photoinduced electron-transfer reaction takes place between the conjugated organic system (electron donor) and TiO_2 (electron acceptor), which effective suppresses the recombination of the photogenerated electron–hole pairs (Luo et al., 2012). Consequently, electrons would be captured by H_2O or oxygen adsorbed on the surface of the photocatalysts to produce $\bullet O_2^-$, which involves in the degradation of MO along with h^+, which conduce to improve the visible light photocatalytic activity of NH_2-Phen/TiO_2, NO_2-Phen/TiO_2, and Phen/TiO_2 nanocomposites.

CONCLUSION

Novel TiO_2-based hybrid photocatalysts containing different delocalized π-conjugated systems (NH_2-Phen/TiO_2, NO_2-Phen/TiO_2, and Phen/TiO_2) and TiO_2 were successfully synthesized *via* the hydrothermal method. Regardless of DRS, photocurrent response, PL, EIS, and photocatalytic degradation of MO, the results demonstrate that delocalized π-conjugated Phen and its derivatives greatly broadened the range of light absorption and effectively promoted the transfer of photogenerated electron–hole pairs; thus, NH_2-Phen/TiO_2, NO_2-Phen/TiO_2, and Phen/TiO_2 exhibited much higher visible light photocatalytic activity than TiO_2. NH_2-Phen/TiO_2 showed the highest photocatalytic performance in the degradation of MO under visible light irradiation, which indicated that introducing a delocalized π-conjugated system with the amino group into TiO_2 was more favorable in improving the photocatalytic activity. This study provides a guide for the synthesis of highly efficient TiO_2-based catalysts at the molecular level.

DATA AVAILABILITY STATEMENT

The original contributions presented in the study are included in the article/**Supplementary Material**; further inquiries can be directed to the corresponding authors.

AUTHOR CONTRIBUTIONS

WZ, JL, and NH contributed to the experiments' operation, data analysis, and writing of the draft manuscript; PC, CF, DW, and YB contributed to the planning and design of both the project and the manuscript.

FUNDING

This work was financially supported by the National Natural Science Foundation of China (grant numbers 41703123, 42077162, and 41573130) and the Fundamental Research Funds for the Central Public-Interest Scientific Institution.

SUPPLEMENTARY MATERIAL

The Supplementary Material for this article can be found online at: https://www.frontiersin.org/articles/10.3389/fchem.2021.700380/full#supplementary-material

REFERENCES

Ardo, S., and Meyer, G. J. (2009). Photodriven Heterogeneous Charge Transfer with Transition-Metal Compounds Anchored to TiO_2 Semiconductor Surfaces. *Chem. Soc. Rev.*, 38, 115–164. doi:10.1039/B804321N

Awfa, D., Ateia, M., Fujii, M., Johnson, M. S., and Yoshimura, C. (2018). Photodegradation of Pharmaceuticals and Personal Care Products in Water Treatment Using Carbonaceous-TiO_2 Composites: a Critical Review of Recent Literature. *Water Res.* 142, 26–45. doi:10.1016/j.watres.2018.05.036

Cai, N., Moon, S.-J., Cevey-Ha, L., Moehl, T., Humphry-Baker, R., Wang, P., et al. An Organic D-π-A Dye for Record Efficiency Solid-State Sensitized Heterojunction Solar Cells. *Nano Lett.* 2011, 11, 1452–1456. doi:10.1021/nl104034e

Cao, J., Xu, B. Y., Luo, B. D., Lin, H. L., and Chen, S. F. (2011). Novel BiOI/BiOBr Heterojunction Photocatalysts with Enhanced Visible Light Photocatalytic Properties. *Catal. Commun.* 13, 63–68. doi:10.1016/j.catcom.2011.06.019

Carbuloni, C. F., Savoia, J. E., Santos, J. S. P., Pereira, C. A. A., Marques, R. G., Ribeiro, V. A. S., et al. (2020). Degradation of Metformin in Water by TiO_2–ZrO_2 Photocatalysis. *J. Environ. Manag.* 262, 110347. doi:10.1016/j.jenvman.2020.110347

Chen, C. C., Ma, W. H., and Zhao, J. C. (2010). Semiconductor-mediated Photodegradation of Pollutants under Visible-Light Irradiation. *Chem. Soc. Rev.* 39, 4206–4219. doi:10.1039/B921692H

Chong, M. N., Jin, B., Chow, C. W., and Saint, C. (2010). Recent Developments in Photocatalytic Water Treatment Technology: a Review. *Water Res.* 44, 2997–3027. doi:10.1016/j.watres.2010.02.039

Cottineau, T., Rouet, A., Fernandez, V., and Brohana, L. (2014). Richard-Plouet M., Intermediate Band in the gap of Photosensitive Hybrid Gel Based on Titanium

Oxide: Role of Coordinated Ligands during Photoreduction. *J. Mater. Chem. A.* 2, 11499–11508. doi:10.1039/C4TA02127D

Dai, Z., Qin, F., Zhao, H. P., Tian, F., Liu, Y. L., and Chen, R. (2015). Time-dependent Evolution of the $Bi_{3.64}$ $Mo_{0.36}O_{6.55}/Bi_2$ MoO_6 Heterostructure for Enhanced Photocatalytic Activity via the Interfacial Hole Migration. *Nanoscale, Nanoscale* 7, 11991–11999. doi:10.1039/C5NR02745D

Dong, W. H., Wu, D. D., Luo, J. M., Xing, Q. J., Liu, H., Zou, J. P., et al. (2017). Coupling of Photodegradation of RhB with Photoreduction of CO_2 over rGO/$SrTi_{0.95}Fe_{0.05}O_{3-\delta}$ Catalyst: A Strategy for One-Pot Conversion of Organic Pollutants to Methanol and Ethanol. *J. Catal.* 349, 218–225. doi:10.1016/j.jcat.2017.02.004

Edvinsson, T., Li, C., Pschirer, N., Scho, N. J., Eickemeyer, F., Sens, R., et al. (2007). Intramolecular Charge-Transfer Tuning of Perylenes: Spectroscopic Features and Performance in Dye-Sensitized Solar Cells. *J. Phys. Chem. C*, 111, 15137–15140. doi:10.1021/jp076447c

Feng, W., Feng, Y., and Wu, Z. (2005). Ultrasonic-Assisted Synthesis of Poly(3-hexylthiophene)/TiO_2 Nanocomposite and its Photovoltaic Characteristics. *Jpn. J. Appl. Phys.* 44 (10), 7494–7499. doi:10.1143/JJAP.44.7494

Fujisawa, J., Eda, T., Giorgi, G., and Hanaya, M. (2017). Visible-to-Near IR Wide-Range Light Harvesting by Interfacial Charge-Transfer Transitions between TiO_2 and P-Aminophenol and Evidence of Direct Electron-Injection to the Conduction Band of TiO_2. *J. Phys. Chem. C* 121 (34), 18710–18716. doi:10.1021/acs.jpcc.7b06012

Fujisawa, J., Matsumura, S., and Hanaya, M. (2016). A Single Ti-O-C Linkage Induces Interfacial Chargetransfer Transitions between TiO_2 and a π-conjugated Molecule. *Chem. Phys. Lett.* 657, 172–176. doi:10.1016/j.cplett.2016.05.049

Gopinath, K. P., Madhav, N. V., Krishnan, A., Malolan, R., and Rangarajan, G. (2020). Present Applications of Titanium Dioxide for the Photocatalytic Removal of Pollutants from Water: a Review. *J. Environ. Manag.* 27, 110906. doi:10.1016/j.jenvman.2020.110906

Grzechulska, D. J., Tomaszewska, M., and Morawski, A. W. (2009). Integration of Photocatalysis with Membrane Processes for Purification of Water Contaminated with Organic Dyes. *Desalination* 241, 118–126. doi:10.1016/j.desal.2007.11.084

Ishikawa, A., Takata, T., Kondo, J. N., Hara, M., Kobayashi, H., and Domen, K. (2002). Oxysulfide $Sm_2Ti_2S_2O_5$ as a Stable Photocatalyst for Water Oxidation and Reduction under Visible Light Irradiation (λ ≤ 650 Nm). *J. Am. Chem. Soc.* 124, 13547–13553. doi:10.1021/ja0269643

Jiang, H., Liu, J., Li, M., Tian, L., Ding, G., Chen, P., et al. (2018). Facile Synthesis of C-decorated Fe, N Co-doped TiO_2 with Enhanced Visible-light Photocatalytic Activity by a Novel Co-precursor Method. *Chin. J. Catal.* 39, 747–759. doi:10.1016/S1872-2067(18)63038-4

Jiang, H., Zhang, W., Chen, P., Zhang, W., Wang, G., Luo, X., et al. (2016). Equipping an Adsorbent with an Indicator: a Novel Composite to Simultaneously Detect and Remove Heavy Metals from Water. *J. Mater. Chem. A.* 4, 11897–11907. doi:10.1039/C6TA04885D

Jono, R., Fujisawa, J., Segawa, H., and Yamashita, K. (2011). Theoretical Study of the Surface Complex between TiO_2 and TCNQ Showing Interfacial Charge-Transfer Transitions. *J. Phys. Chem. Lett.* 2, 1167–1170. doi:10.1021/jz200390g

Kandiel, T. A., Robben, L., Alkaim, A., and Bahnemann, D. (2013). Brookite versus Anatase TiO_2 Photocatalysts: Phase Transformations and Photocatalytic Activities. *Photochem. Photobiol. Sci.* 12, 602–609. doi:10.1039/c2pp25217a

Kaur, S., and Singh, V. (2007). Visible Light Induced Sonophotocatalytic Degradation of Reactive Red Dye 198 Using Dye Sensitized TiO_2. *Ultrason. Sonochem.* 14, 531–537. doi:10.1016/j.ultsonch.2006.09.015

Kim, K. H., Jahan, S. A., Kabir, E., and Brown, R. J. (2013). A Review of Airborne Polycyclic Aromatic Hydrocarbons (PAHs) and Their Human Health Effects. *Environ. Int.* 60, 71–80. doi:10.1016/j.envint.2013.07.019

Kubacka, A., Garcia, M. F., and Colon, G. (2012). Advanced Nanoarchitectures for Solar Photocatalytic Applications. *Chem. Rev.* 112, 1555–1614. doi:10.1021/cr100454n

Li, S., Sun, S., Wu, H., Wei, C., and Hu, Y. (2018). Effects of Electron-Donating Groups on the Photocatalytic Reaction of MOFs Catal. *Sci. Technol.* 8, 1696–1703. doi:10.1039/C7CY02622F

Li, X. P., Shen, G., Jin, X., Liu, M., Shi, L., et al. (2016). Novel Polyimide Containing 1,10-phenanthroline and its Europium (III) Complex: Synthesis, Characterization, and Luminescence Properties. *J. Mater. Sci.* 51, 2072–2078. doi:10.1007/s10853-015-9517-8

Li, Z., Zhang, L., Liu, Y., Shao, C., Gao, Y., Fan, F., et al. (2020). Surface-Polarity-Induced Spatial Charge Separation Boosts Photocatalytic Overall Water Splitting on GaN Nanorod Arrays. *Angew. Chem. Int. Ed.* 59, 935. doi:10.1002/anie.201912844

Liu, G., Yang, H. G., Wang, X., Cheng, L., Pan, J., Lu, G. Q., et al. (2009). Visible Light Responsive Nitrogen Doped Anatase TiO2 Sheets with Dominant {001} Facets Derived from TiN. *J. Am. Chem. Soc.* 131, 12868–12869. doi:10.1021/ja903463q

Luo, Q., Bao, L., Wang, D., Li, X., and An, J. (2012). Preparation and Strongly Enhanced Visible Light Photocatalytic Activity of TiO2 Nanoparticles Modified by Conjugated Derivatives of Polyisoprene. *J. Phys. Chem. C* 116 (49), 25806–25815. doi:10.1021/jp308150j

Luo, X. B., Deng, F., Min, L. J., Luo, S. L., Guo, B., Zeng, G. S., et al. (2013). Facile One-step Synthesis of Inorganic-Framework Molecularly Imprinted TiO_2/WO_3 Nanocomposite and its Molecular Recognitive Photocatalytic Degradation of Target Contaminant. *Environ. Sci. Technol.* 47, 7404–7412. doi:10.1021/es4013596

Margalias, An., Seintis, K., Yigit, M. Z., Can, M., Sygkridou, D., Giannetas, V., et al. (2015). The Effect of Additional Electron Donating Group on the Photophysics and Photovoltaic Performance of Two New Metal Free D-π-A Sensitizers. *Dyes Pigm.* 121, 316–327. doi:10.1016/j.dyepig.2015.05.028

Murgolo, S., Ceglie, C., Iaconi, C., and Mascolo, G. (2021). Novel TiO_2-Based Catalysts Employed in Photocatalysis and Photoelectrocatalysis for Effective Degradation of Pharmaceuticals (PhACs) in Water: A Short Review. *Curr. Opin. Green Sust. Chem.* 30, 100473. doi:10.1016/j.cogsc.2021.100473

Pang, Y. L., Lim, S., Ong, H. C., et al. (2016). Research Progress on Iron Oxide-Based Magnetic Materials: Synthesis Techniques and Photocatalytic Applications. *Ceramics Int.* 42 (1), 9–34. doi:10.1016/j.ceramint.2015.08.144

Ramakrishna, G., and Ghosh, H. N., (2002). Efficient Electron Injection from Twisted Intramolecular Charge Transfer (TICT) State of 7- Diethyl Amino Coumarin 3-Carboxylic Acid (D-1421) Dye to TiO_2 Nanoparticle. *J. Phys. Chem. A.* 106, 2545–2553. doi:10.1021/jp021298d

Shao, Y., Cao, C. S., Chen, S. L., He, M., Fang, J. L., Chen, J., et al. (2015). Investigation of Nitrogen Doped and Carbon Species Decorated TiO2 with Enhanced Visible Light Photocatalytic Activity by Using Chitosan. *Appl. Catal. B* 179, 344–351. doi:10.1016/j.apcatb.2015.05.023

Shibano, Y., Umeyama, T., and MatanoHiroshi Imahori, Y. H. (2007). Electron-Donating Perylene Tetracarboxylic Acids for Dye-Sensitized Solar Cells. *Org. Lett.* 9 (10), 1971–1974. doi:10.1021/ol070556s

Soner Çakar, S. (2019). 1,10 Phenanthroline 5,6 Diol Metal Complex (Cu, Fe) Sensitized Solar Cells: A Cocktail Dye Effect. *J. Power Sourc.* 435, 226825. doi:10.1016/j.jpowsour.2019.226825

Tian, H., Yang, X., Pan, J., Chen, R., Liu, M., Zhang, Q., et al. (2008). A Triphenylamine Dye Model for the Study of Intramolecular Energy Transfer and Charge Transfer in DyeSensitized Solar Cells. *Adv. Funct. Mater.* 18, 3461–3648. doi:10.1002/anie.201590015

Verma, S., and Ghosh, H. N. (2014). Tuning Interfacial Charge Separation by Molecular Twist: A New Insight into Coumarin-Sensitized TiO_2 Films. *J. Phys. Chem. C* 118 (20), 10661–10669. doi:10.1021/jp5023696

Wei, T., Zeng, Y., Hong, L., Zhang, H., Wang, G., and Wang, S. (2018). Experimental and Theoretical Investigations of the Optoelectronic Properties of a 1,2,5-Oxadiazolo-Fused Phenanthroline. *Monatsh Chem.* 149, 1753–1758. doi:10.1007/s00706-018-2210-2

Wu, K., Wu, P., Zhu, J., Liu, C., Dong, X., Wu, J., et al. (2018). Synthesis of Hollow Core-Shell CdS@TiO_2/Ni_2P Photocatalyst for Enhancing Hydrogen Evolution and Degradation of MB. *Chem. Eng. J.* 360. 221–230. doi:10.1016/j.cej.2018.11.211

Xie, C., Hu, X., Guan, Z., Li, X. D., Zhao, F., Song, Y., et al. (2020). Tuning the Properties of Graphdiyne by Introducing Electron-Withdrawing/Donating Groups. *Angew. Chem. Int. Ed.* 59, 13542–13546. doi:10.1002/anie.202004454

Xu, L., Yang, L., Johansson, E. M. J., Wang, Y., Jin, P., et al. (2018). Photocatalytic activity and mechanism of bisphenol a removal over TiO_{2-x}/rGO nanocomposite driven by visible light. *Chem. Eng. J.* 350, 1043–1055. doi:10.1016/j.cej.2018.06.046

Xu, P., Lu, J., Xu, T., Gao, S. U., Huang, B. B., and Dai, Y. (2010). I_2-Hydrosol-Seeded Growth of (I_2) N-C-Codoped Meso/Nanoporous TiO_2 for Visible Light-Driven Photocatalysis. *J. Phys. Chem. C* 114, 9510–9517. doi:10.1021/jp101634s

Xu, Y., Zhang, H., Liu, Q., Liu, J., Chen, R., Yu, J., et al. (2021). Surface Hybridization of π-conjugate Structure Cyclized Polyacrylonitrile and Radial Microsphere Shaped TiO_2 for Reducing U(VI) to U(IV). *J. Hazard. Mater.*, 416. 125812. doi:10.1016/j.jhazmat.2021.125812

Xun, S., Ti, Q., Jiao, Z., He, M., Chen, L., Zhu, L., et al. (2008). Dispersing TiO_2 Nanoparticles on Graphite Carbon for an Enhanced Catalytic Oxidative Desulfurization Performance. *Ind. Eng. Chem. Res.* 59 (41), 18471–18479. doi:10.1021/acs.iecr.0c03202

Yang, X., Li, Y., Zhang, P., Zhou, R., Peng, H., Liu, D., et al. (2018). Photoinduced in situ deposition of uniform and well-dispersed PtO_2 nanoparticles on ZnO nanorods for efficient catalytic reduction of 4-Nitrophenol. *ACS Appl. Mater. Inter.* 10, 23154–23162. doi:10.1021/acsami.8b06815

Zhang, G. A., and Cheng, Y. F. (2009). Micro-electrochemical Characterization and Mott–Schottky Analysis of Corrosion of Welded X70 Pipeline Steel in Carbonate/bicarbonate Solution. *Electrochimica Acta* 55, 316–324. doi:10.1016/j.electacta.2009.09.001

Zhou, F., Shi, R., and Zhu, Y. (2011). Significant Enhancement of the Visible Photocatalytic Degradation Performances of γ-Bi_2MoO_6 Nanoplate by Graphene Hybridization. *J. Mol. Catal. A, Chem.* 340, 77–82. doi:10.1016/j.molcata.2011.03.012

Zhou, G., Wu, M. F., Xing, Q. J., Li, F., Liu, H., Luo, X. B., et al. (2018). Synthesis and Characterizations of Metal-free Semiconductor/MOFs with Good Stability and High Photocatalytic Activity for H_2 Evolution: A Novel Z-Scheme Heterostructured Photocatalyst Formed by Covalent Bonds. *Appl. Catal. B* 220, 607–614. doi:10.1016/j.apcatb.2017.08.086

Zou, J. P., Wu, D. D., Luo, J. M., Xing, Q. J., Luo, X. B., Dong, W. H., et al. (2016). A Strategy for One-Pot Conversion of Organic Pollutants into Useful Hydrocarbons through Coupling Photodegradation of MB with Photoreduction of CO_2. *ACS Catal.* 6, 6861–6867. doi:10.1021/acscatal.6b01729

Conflict of Interest: The authors declare that the research was conducted in the absence of any commercial or financial relationships that could be construed as a potential conflict of interest.

Publisher's Note: All claims expressed in this article are solely those of the authors and do not necessarily represent those of their affiliated organizations, or those of the publisher, the editors and the reviewers. Any product that may be evaluated in this article, or claim that may be made by its manufacturer, is not guaranteed or endorsed by the publisher.